Available online at www.sciencedirect.com
SCIENCE DIRECT
Intermetallics 12 (2004) 1373–1380
Intermetallics
www.elsevier.com/locate/intermet

Mixed site occupancies in the μ phase

J.-M. Joubert[a,*], N. Dupin[b]

[a]Laboratoire de Chimie Métallurgique des Terres Rares, ISCSA, CNRS, UPR 209, 2-8 rue Henri Dunant, F-94320 Thiais Cedex, France
[b]Calcul Thermodynamique, 3 rue de l'Avenir, F-63670, Orcet, France

Received 24 February 2004; received in revised form 17 March 2004; accepted 12 April 2004
Available online 21 July 2004

Abstract

The μ phase has been studied in different systems (Ta–Ni, Mo–Co, Nb–Ni) as a function of the composition. In addition, its stability in the Mn–Si system has been investigated. The atom distribution on the five different sites of the crystal structure has been obtained from Rietveld refinement of X-ray powder diffraction data. These experimental data are compared to the values computed from first principles results and from existing Calphad assessments of the different systems. Conclusions are drawn concerning the model to be chosen for describing this phase.

Keywords: A. Intermetallics, miscellaneous; B. Crystallography; D. Site occupancy; E. Phase diagram, prediction; F. Diffraction (electron, neutron and X-ray)

1. Introduction

The μ phase is a hard-brittle intermetallic compound showing up in various systems involving transition metals. It may appear in industrial Ni-, Co- or Fe-based alloys in which early 4d or 5d refractory metals (Nb, Ta, Mo, W) act as strengthening elements. It is detrimental because its precipitation induces a local depletion of the matrix in these alloying elements and its needle morphology can easily initiate rupture. Its presence should be avoided, or, at least, carefully controlled. Therefore, its range of stability should be accurately studied, in particular with the Calphad approach well adapted to the modelling of multicomponent systems. The μ phase has recently been shown to be able to store reversibly significant amount of hydrogen in different systems [1,2].

At present, the μ phase has been reported and confirmed to exist in 12 binary A–B systems, where A is a 4d or 5d element among Nb, Ta, Mo or W, and B is a 3d element among Fe, Co, Ni or Zn. Its crystal structure is typified by W_6Fe_7 compound which crystallizes in the space group $R\bar{3}m$ with an ideal atomic distribution among the sites as follows (in hexagonal setting): W in sites $6c_1$ (0, 0, 0.167), $6c_2$ (0, 0, 0.346), $6c_3$ (0, 0, 0.448), and Fe in sites $3a$ (0, 0, 0) and $18h$ $(0.833, \bar{x}, 0.167)$ [3]. This model, with full occupancy of each site by one given atom, allows to describe a composition of 46.2 at.% A which will be referred to as the stoichiometric or ideal composition in the following text. However, the μ phase is characterized by a large non-stoichiometry. In Fig. 1, has been plotted its reported homogeneity range for the different systems in which it appears (no data are available concerning the homogeneity range of the Ta–Zn μ phase). The homogeneity domain is often quite large (up to 12 at.%). The deviation from the ideal composition may occur both towards A-rich and A-poor sides. The μ phase exists at its ideal composition only in a few systems (Ta–Co, W–Co, Mo–Co). Only scarce data [4–6] exist on the accommodation of the non-stoichiometry in this phase. Those authors all studied only one composition and proposed atom mixing on a single site ($3a$). This only defect does not allow describing the composition ranges observed in all the systems, in particular in Ta–Ni, Nb–Ni and Ta–Co.

Ansara et al. [7] discussed the different Calphad models of the μ phase reported in the literature. The ability of these models to describe the different systems where this phase appears was commented with respect to the available phase diagram and crystallographic data. The lack of truthful experimental data in many systems was enlighted. Joubert and Feutelais [8] presented site occupancies obtained from the Rietveld refinement for five different compositions of

* Corresponding author. Tel.: +33-1-49-78-1211; fax: +33-1-49-78-1203.
E-mail address: jean-marc.joubert@glvt-cnrs.fr (J.-M. Joubert).

0966-9795/$ - see front matter © 2004 Elsevier Ltd. All rights reserved.
doi:10.1016/j.intermet.2004.04.036

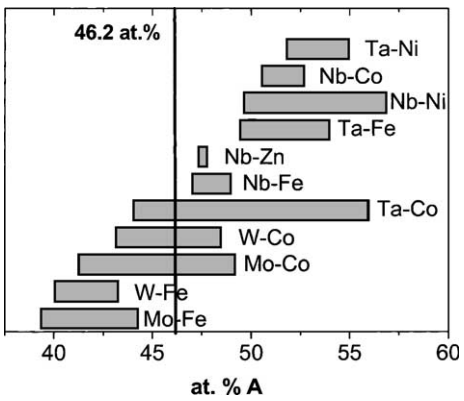

Fig. 1. Homogeneity range of the known binary μ phases [26] ([8] for Nb–Ni system). No data concerning the homogeneity domain are available for the Ta–Zn μ phase.

the μ phase in the system Nb–Ni. The mixing on site 3*a* was confirmed but also shown on sites $6c_3$ and 18*h*. Their approach is here extended to other systems with the following aims: (i) determine accurate stability ranges in several systems, (ii) determine the atomic distribution on the different sites by crystallographic methods, and (iii) propose a coherent model for the Calphad description of the μ phase in the whole concentration range where the phase exists in different systems.

In addition to Nb–Ni system in which the highest composition of the A element is reported, another system extending on the A-rich side, Ta–Ni, was chosen. Among the systems for which the μ phase exists in A-poor region, Mo–Co was studied because it also allows studying the μ phase at the stoichiometric composition. Finally, a μ phase was reported to exist in the Mn–Si system at the composition Mn_6Si at 600 °C by Gladyshevskii et al. [9]. However, the existence of this phase was not confirmed, and it was not taken into account in subsequent reviews of the system [10]. A careful investigation was therefore conducted in this area.

2. Experimental

The experimental procedure used was the same for Ta–Ni and Mo–Co alloys. Due to the high melting point of the A element, they were synthesized by arc melting of the pure elements (Ta 99.9%, Ni 99.9%, Mo 99.9%, Co 99.99%) under argon atmosphere. Equilibrated alloys were obtained after 13 days at 1200 °C (Ta–Ni) or 38 days at 1150 °C (Mo–Co) annealing treatments. The compositions studied were chosen in the two adjacent two-phase fields and in the single phase region. This allows obtaining the crystallographic properties of the μ phase as a function of composition in the whole homogeneity range, in a temperature region where it is expected to be the largest. Mn–Si (Mn 99.98%, Si 99.999%) alloys were induction melted under argon atmosphere and equilibrated at 600 °C for 32 days. Whatever the system, the equilibration treatment took place in a silica tube sealed under vacuum (Mo–Co) or argon (Ta–Ni, Mn–Si) atmosphere. The alloys were protected from a possible reaction with silica by a tantalum foil with which no reaction was observed, and quenched by throwing the silica tube in cold water.

The μ phase composition as well as the composition of the secondary phase, when possible, was obtained by electron probe microanalysis (EPMA—Camebax SX100). All the samples were sufficiently brittle to be reduced easily to powder in an agate mortar. The powder was deposited on a doublesided adhesive tape. X-ray diffraction measurements were performed at room temperature with a Philips PW1710 diffractometer equipped with a rear graphite monochromator with Cu K_α radiation. Rietveld analysis of the powder diffraction data was conducted with the program Fullprof [11]. The secondary phase, when present, was included in the refinement with its crystal structure from the literature data. The refinement procedure was identical to the one adopted in the study of the Nb–Ni μ phase [8]. Contrary to what occurred in that system, no significant preferential orientation was observed and the related parameters were therefore not refined. As previously described, the lattice parameters, the variable coordinates and the occupancy parameters at each site could be obtained. For these latter parameters, and as previously explained, the total amount of each element was constrained to match the analyzed composition of the phase as measured by EPMA. This is sufficient to adjust the scale factor and allows refining the distribution of the elements over the five sites. The estimated standard deviations of the lattice parameters and of the atomic positions have been multiplied by the so-called Bérar's factor (~2).

3. Results

The numerical results concerning all the alloys are presented in Table 1. The analyzed composition of the μ phase measured by EPMA, together with the one of the second phase in equilibrium, when it exists and when it has been possible to analyze it, are presented. The lattice parameters, atomic coordinates and occupancy parameters at the different sites are listed. An example of refinement is given in Fig. 2.

3.1. Ta–Ni

Secondary phases were observed for the samples synthesized outside the homogeneity domain of the μ phase. As expected from the phase diagram [12], the two phases in equilibrium with the μ phase are $TaNi_2$ with the $MoSi_2$ structure type on the Ta-poor side, and Ta_2Ni with Al_2Cu structure type on the Ta-rich side. Both phases were observed in the diffraction patterns and were taken into account in the refinement. They were both analyzed by

Table 1
Rietveld refinement results for the μ phase in each sample

Nominal composition	$Ta_{47}Ni_{53}$	$Ta_{52.5}Ni_{47.5}$	$Ta_{57}Ni_{43}$	$Mo_{38}Co_{62}$	$Mo_{46.15}Co_{53.85}$	$Mo_{52}Co_{48}$	$Mn_{85}Si_{15}$
μ-Phase composition	$Ta_{51.8(3)}Ni_{48.2(3)}$	$Ta_{53.1(7)}Ni_{46.9(7)}$	$Ta_{55.0(6)}Ni_{45.0(6)}$	$Mo_{40.7(2)}Co_{59.3(2)}$	$Mo_{45.3(2)}Co_{54.7(2)}$	$Mo_{48.1(2)}Co_{51.9(2)}$	$Mn_{84.7(1)}Si_{15.3(1)}$
a (Å)	4.899(1)	4.911(1)	4.929(1)	4.738(1)	4.761(1)	4.776(1)	4.693(1)
c (Å)	26.764(7)	26.836(6)	26.967(3)	25.484(4)	25.590(4)	25.697(6)	25.571(1)
V (Å^3)	556.4(3)	560.4(2)	567.5(1)	495.5(2)	502.4(1)	507.6(2)	487.6(1)
z_{6c1}	0.1651(4)	0.1654(3)	0.1652(2)	0.1655(3)	0.1656(2)	0.1649(3)	0.1662(4)
z_{6c2}	0.3440(4)	0.3444(3)	0.3460(2)	0.3483(3)	0.3474(2)	0.3467(3)	0.3476(4)
z_{6c3}	0.4498(5)	0.4502(4)	0.4507(2)	0.4521(4)	0.4518(2)	0.4521(5)	0.4554(4)
x_{18h}	0.8305(37)	0.8373(24)	0.8380(18)	0.8379(15)	0.8356(10)	0.8314(19)	0.8363(12)
z_{18h}	0.2552(7)	0.2555(6)	0.2559(4)	0.2561(5)	0.2560(3)	0.2556(5)	0.2554(25)
A occupancy 3a (atom/fractional)	2.67(4)/0.889(14)	2.44(3)/0.814(10)	2.30(4)/0.768(12)	0.10(6)/0.033(19)	0.60(4)/0.201(12)	1.92(6)/0.638(21)	3/1
A occupancy 6c_1 (atom/fractional)	5.67(5)/0.945(8)	5.76(4)/0.960(7)	6/1	5.23(8)/0.872(14)	5.70(5)/0.950(8)	5.46(8)/0.910(13)	6/1
A occupancy 6c_2 (atom/fractional)	5.41(6)/0.901(8)	5.82(4)/0.971(7)	5.83(6)/0.972(10)	6.01(8)/1.002(14)	5.90(5)/0.984(8)	6.01(10)/1.002(15)	6/1
A occupancy 6c_3 (atom/fractional)	4.63(6)/0.771(8)	5.15(4)/0.859(7)	5.72(5)/0.954(9)	4.56(7)/0.760(12)	5.28(5)/0.881(8)	4.32(8)/0.720(13)	5.60(7)/0.933(12)
A occupancy 18h (atom/fractional)	1.83(6)/0.102(2)	1.54(4)/0.086(3)	1.60(5)/0.089(3)	−0.02(8)/−0.001(4)	0.18(5)/0.010(3)	1.06(8)/0.059(4)	12.55(7)/0.697(4)
Second phase (wt%)	$Ta_{34.4(2)}Ni_{65.6(2)}$ $MoSi_2$ type (a = 3.154 Å, c = 7.904 Å) (19 wt%)	–	$Ta_{\sim 66.7}Ni_{\sim 33.3}$ Al_2Cu type (a = 6.190 Å, c = 4.866 Å) (19 wt%)	$Mo_{19.0(1)}Co_{81.0(1)}$[a] hcp(a = 2.559 Å, c = 4.125 Å) (9 wt%)	–	bcc (a = 3.147 Å) (11 wt%)	R phase (a = 10.885 Å, c = 19.168 Å) (38 wt%)
R_p (%)	16.8	14.4	16.4	14.0	9.5	13.2	13.6
χ^2	5.0	4.3	2.0	3.7	4.1	3.6	4.6
R_B (%)	10.0	7.4	7.8	5.8	4.9	6.1	5.3

Indicated: the nominal composition, the μ phase composition as obtained by EPMA, the lattice parameters in the hexagonal description, the variable atomic coordinates, A (Ta, Mo or Mn) atom occupancies on the five sites (in atom per site and fractional), the nature and quantity of the secondary phase when present, and conventional Rietveld agreement factors on whole diagram (R_p, background corrected) and on the integrated intensities of reflections corresponding to the μ phase (R_B), as well as the goodness of fit (χ^2). Estimated standard deviations referring to the last digit are indicated between parentheses.

[a] Analyzed in another sample of composition $Mo_{33.3}Co_{66.7}$ (see text).

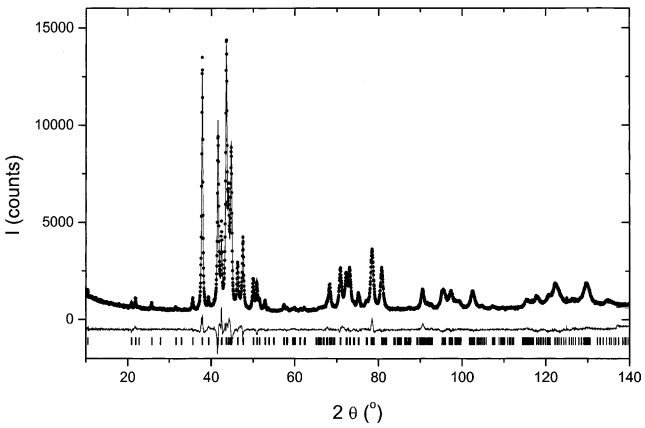

Fig. 2. Rietveld plot of the sample $Mo_{46.15}Co_{53.85}$. Observed (dots) and calculated (full lines) curves with difference curve below. Line positions are indicated by vertical bars.

EPMA but a reliable compositional analysis could only be obtained for $TaNi_2$, due to a very thin structure of the precipitates of Ta_2Ni. In each case the amount of the secondary phase obtained by the X-ray analysis is in agreement with the values expected from the lever rule. The limits of the homogeneity domain of the μ phase at 1200 °C, the heat treatment temperature, are given by the EPMA analysis of those two two-phase samples: 51.8 and 55.0 at.% Ta. These limits are in relatively good agreement with previous measurements of diffusion couples at the same temperature (50.7–55.3 [13], 50.5–54.2 [14]). *a* and *c* lattice parameters show a perfectly linear increase as a function of analyzed tantalum composition (Fig. 3), which testifies for the accuracy of both measurements. Concerning the occupancy parameters, one should note that the estimated standard deviations are typically twice less than those obtained previously on the Nb–Ni μ phase. This is due to the higher diffraction contrast (difference of the number of electrons) between A and B atoms in the present case.

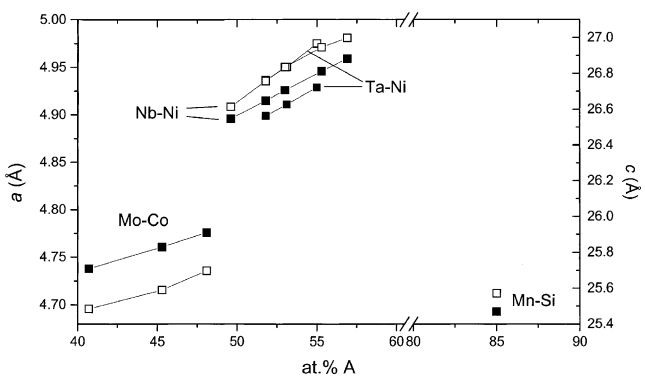

Fig. 3. Lattice parameters of the μ phase as a function of the A atom composition (A = Ta, Mo, Mn, Nb) for the different systems investigated (*a*, solid symbols; *c*, open symbols) together with the data on Nb–Ni system [8].

3.2. Mo–Co

The second phase in equilibrium with the μ phase on the Mo poor side can be refined as a disordered hcp phase in agreement with the phase diagram at the equilibrium temperature [15]. The weak quantity and the fine microstructure of that phase in the two phase sample do not allow a reliable EPMA analysis. However, the study of another sample of composition $Mo_{33.3}Co_{66.7}$ at the same temperature yields a composition $Mo_{19.0(1)}Co_{81.0(1)}$. In this latter sample no superstructure lines corresponding to the Ni_3Sn type low temperature phase are detected confirming the phase diagram as described by Quinn and Hume-Rothery in this region [16]. On the Mo-rich side, the bcc phase was found to be the equilibrium phase at 1150 °C. This result is in contradiction with the results of Heijwegen and Rieck [17] (chosen by Davydoff and Kattner in their evaluation of the system [15]) who found a detectable layer corresponding to the σ phase down to 1000 °C in diffusion couples. On the other hand, it agrees with the result of Quinn and Hume-Rothery [16] who studied equilibrated alloys by X-ray and metallographic analysis, and determined the eutectoid decomposition temperature of σ to be between 1240 and 1280 °C. The hcp and bcc phase content refined from X-ray diffraction is in perfect agreement with a lever rule calculation based on analyzed compositions.

The limits of the homogeneity domain are 40.7–48.1 at.% Mo. They are in reasonable agreement with the limits determined by Heijwegen and Rieck [17] from diffusion couples measurements (41.5–48.6 at.% Mo at the same temperature). The lattice parameters of the μ phase show, like in the Ta–Ni system, a linear increase as a function of the A (Mo) atom content (Fig. 3).

3.3. Mn–Si

A μ phase was previously reported to exist at the composition 85.7 at.% Mn at the same temperature (600 °C) by Gladyshevskii et al. [9] from X-ray diffraction analysis and found to be in equilibrium with the R phase ($R\bar{3}$, *hR53*, $Co_5Cr_2Mo_3$ prototype [18]) on the Mn rich side and with the *ν* phase (*Immm*, *oI186*, Mn_4Si prototype [19]) on the Mn poor side. This phase has not been reported by Wieser and Forgeng [20] in a careful investigation of the phase diagram by X-ray and metallographic analyses, even at this same temperature. The report of Gladyshevskii et al. was not mentioned in further evaluation of the system [10].

The presence of a μ phase was observed in the present work. It was found in four different samples of compositions between 84.5 and 86.1 at.% Mn annealed at 600 °C to be in equilibrium with the R phase. The exact composition is believed to stand in the range 84–85 at.% Mn. It is presently not known how this phase forms and its temperature existence range.

The discrepancies between literature data can be explained by the close composition between the different

phases in that region of the phase diagram. There seems actually to be three different equilibrium phases in less than 6 at.% composition range and the quite complicated crystal structures of those phases give rise to a huge number of overlapping diffraction peaks. A possible narrow temperature existence range of the μ phase could increase these difficulties. Finally, the fact that, in all the samples studied, this phase seems in equilibrium with the R phase could be explained by a pollution. One of these phases could then actually be a ternary phase. Further studies are undergoing in order to check this possibility.

The occurrence of a μ phase at this composition allows extending considerably the actual range of existence of the μ phase towards very high A content. The position in the periodic table of the constituting elements is rather unusual. Mn is the only A type element belonging to the 3d raw. Si is the only B type element belonging to p group though substantial amounts of Al, for example, may be substituted in the Nb–Ni μ phase, or are present in the purely ternary Zr–Nb–Al μ phase. Finally, the Mn–Si μ phase is the only example with a so small radius difference between A and B elements

3.4. μ Phase behaviour

The atomic coordinates show very slight variations as a function of composition in a system and between the different systems, which testifies for small rearrangements in the cell. The lattice parameters of the different samples are presented in Fig. 3 as a function of the composition and are compared with the values obtained in Nb–Ni system [8]. As already noticed, a linear increase is observed in each system in which several compositions were synthesized, which is consistent with the increase of the concentration of the atom with the largest radius (A). The occupancy parameters of the five sites of the crystal structure are plotted in Fig. 4, and will be discussed in Section 4. Sluiter et al. [21] have calculated the site occupancies of the Nb–Ni μ phase from first principles (FP) by applying Connolly Williams Method-Cluster Variation Method. Those results are also shown for comparison. Similar results were also obtained in the Bragg–Williams approximation [22].

4. Discussion

The discussion will focus on the conclusions that can be drawn from the measurement of the occupancy parameters in the various systems, including Nb–Ni system previously investigated [8]. The results of Fig. 4 indicate a relative absence of scatter not only within one given system but also between the different systems. This self-consistency testifies, in a certain extent, for the validity of the measurements, and, on the other hand, suggests the possibility to rationalize the site-occupancy behaviour as a function of composition, whatever the system.

The average occupancy of the different sites follows the rule stating that the largest atoms (A) should occupy preferentially sites with high coordination numbers (CN) [7]. Accordingly, we observe the following order: $6c_2$ (CN = 16), $6c_1$ (CN = 15), $6c_3$ (CN = 14), $3a$ (CN = 12) and $18h$ (CN = 12). A distinction should, however, be made between the two sites with coordination 12 because they have different coordination environments which may explain strongly different behaviour regarding site occupancies. Site $18h$ is coordinated by 5 atoms in positions $6c$, while site $3a$ is coordinated by 6 atoms in positions $6c$. As suggested by Sluiter et al. [21], the conversion of one $18h$ atom from Ni to Nb would result in a loss of Ni–Nb bounds, contrary to what would occur for the conversion of one $3a$ atom which appears to be less energetically favourable.

A sharp transition is observed to occur for A site occupancy in site $3a$ around 46 at.% A. This site is mainly occupied by A (resp. B) for alloys richer (resp. poorer) in A. From what is reported in Fig. 1, the μ phases can be divided into three groups: (i) those existing only at A rich composition which will ever present, whatever the composition, a dominant A occupancy on site $3a$ (in this study Ta–Ni, Nb–Ni, Mn–Si), (ii) those existing only at A poor composition (W–Fe, Mo–Fe), and (iii) those crossing the transition range and which presents, depending on the composition, both A rich or A poor composition on site $3a$ (typified by Mo–Co studied in this work). The three systems belonging to this third group all contain cobalt and have the largest homogeneity domains.

The region of transition is not far from the so-called ideal composition $B_3A_6A_6A_6B_{18}$ and could be roughly represented by a transition between this latter composition and $A_3A_6A_6A_6B_{18}$. No preferred ideal composition can therefore be chosen to describe all the μ phases, since one is valid for group (i), another for group (ii), and both, depending on the composition, for group (iii). In addition, more subtle details are taking place. First, the transition does not seem exactly located around 50 at.% as would be expected in the case of an ideal $B_3A_6A_6A_6B_{18}$ to $A_3A_6A_6A_6B_{18}$ transition. Second, site $3a$ does not seem fully occupied even for compositions up to 56.9 at.% (Nb–Ni), and, finally, site $6c_3$ remains partly disordered whatever the composition. It even seems to be still disordered in the Mn–Si μ phase. On the other hand, sites $6c_1$ and $6c_2$ are almost completely ordered whatever the composition and site $18h$ seems to follow a regular increase of A filling from 41 to 86 at.% A.

It is therefore observed that not one, but several sites can be substantially disordered at a given composition and at the studied temperatures. The state is less ordered than what was calculated after a conventional Calphad description of the μ phase using the compound energy model [14,15,23] or after FP calculations [21]. As noticed by Sluiter et al. [21] in the study of the Nb–Ni system, 2000–3000 K are needed to compute the same amount of disorder as measured. These authors conclude that either the alloys used in

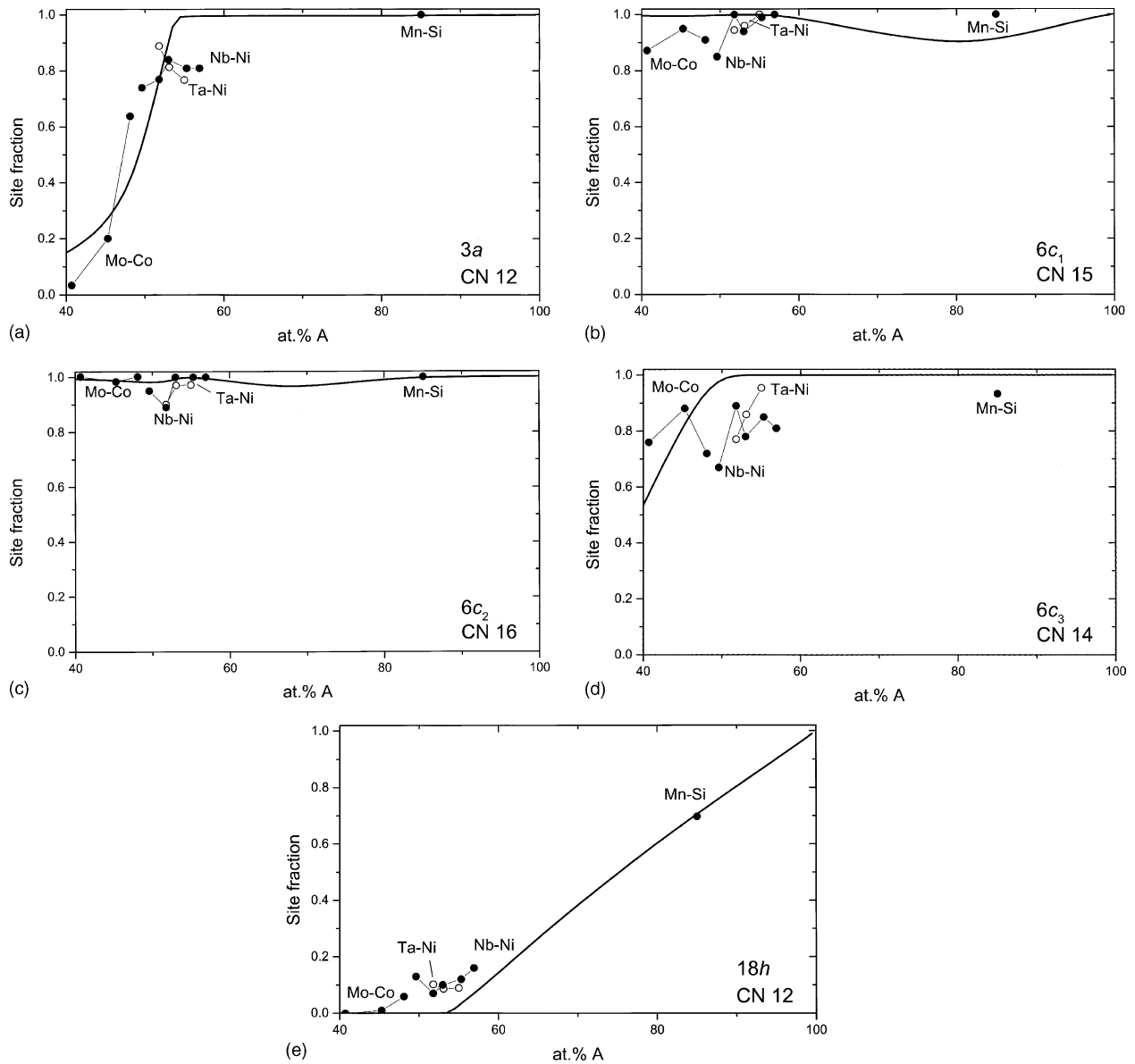

Fig. 4. (a–e) A (A = Ta, Mo, Mn, Nb) occupancy parameters on the 5 sites of the μ phase crystal structure as a function of A composition for the different systems investigated (Ta–Ni: open symbols) together with the data on Nb–Ni system [8]. The experimental data are compared to the calculated site occupancies in Nb–Ni system from FP calculations (solid lines) [21].

the experimental work have not reached equilibrium after 10–30 days annealing treatment at 1273 K, or the theoretical calculations have underestimated entropic effects, such as vibrational effects. The uncertainty of the refinement could also be discussed based on the rather erratic variation of the occupation of site 3*a*, in Ta–Ni system for instance. The validity of measurements done at room temperature for establishing the actual site distribution at high temperature, or the efficiency of the quenching process can also be contested. The relatively low order observed is in favour of an actual measurement of the high temperature structural properties.

Comparison can be done between the measured data and the ones computed from recent Calphad assessment of the related systems (Fig. 5 for Nb–Ni system [23]; Fig. 6 for Mo–Co [15] and Ta–Ni [14] systems). The description of the Nb–Ni μ phase with the model $(Ni,Nb)_{21}Nb_{18}$ (Fig. 5, [23]) fails completely to describe the actual behaviour because the authors consider equal occupancy on the two sites 3*a* and 18*h* which is shown to be inappropriate. Among others, a similar model $(Mo,Co)_{21}(Co,Mo)_{18}$ was used by Davydov and Kattner [15] to describe the Mo–Co μ phase. This one is of course not satisfactory for the same reason as well as another one used: $(Co,Mo)_{21}(Mo,Co)_{12}$ Mo_6. The last model tested by Davydov and Kattner: $(Co,Mo)_3(Mo,Co)_6$ $Mo_{12}Co_{18}$ does not show this drawback (Fig. 6).

This model $(B,A)_3(A,B)_6$ $A_{12}B_{18}$ also used by Cui and Jin [14] in Ta–Ni system is compared to experimental occupancies in Fig. 6. It describes quite well the site occupancies observed as a function of composition. But it

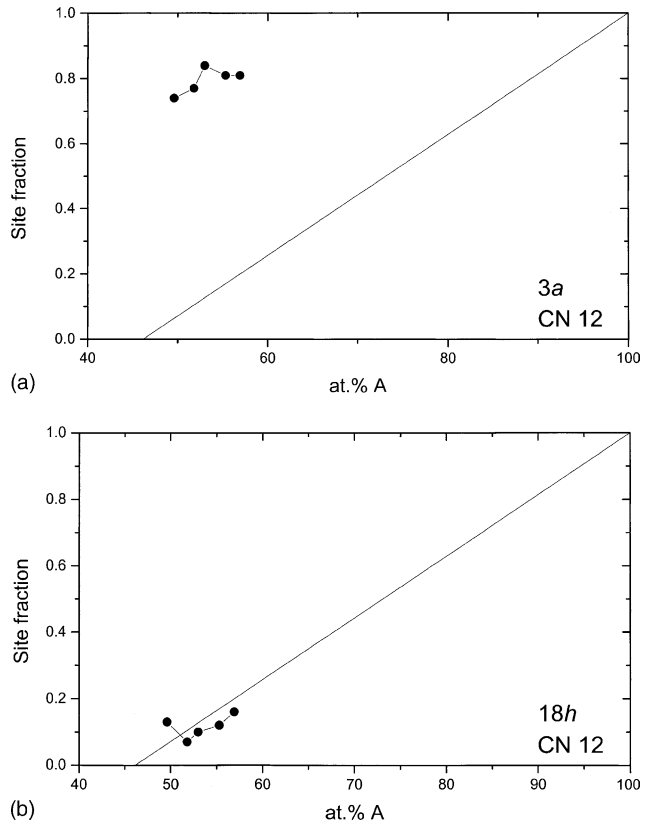

Fig. 5. (a, b) Comparison of the experimental site fractions with the data computed from the assessment of Nb–Ni system (solid lines) [23]. In this assessment the following model was considered: $(A,B)_{21}A_6A_6A_6$. This model allows to describe compositions in the range 46.2–100 at.% A, assumes full occupancy on sites $6c_1$, $6c_2$ and $6c_3$ and equal occupancy on sites 3*a* and 18*h*.

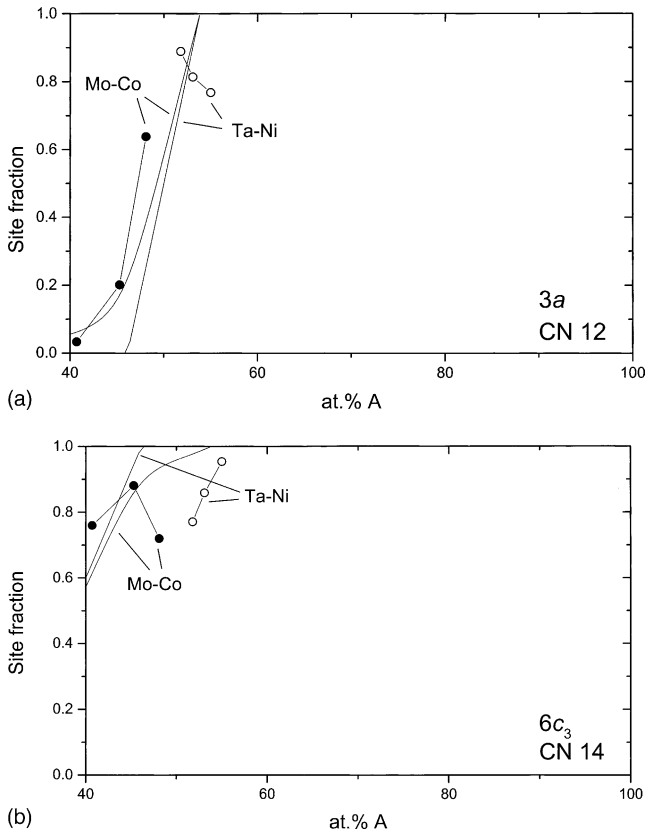

Fig. 6. (a, b) Comparison of the experimental site fractions with the data computed from the assessment of Mo–Co [15] and Ta–Ni [14] system (solid lines). In both assessments the following model was considered: $(A,B)_3(A,B)_6A_6A_6B_{18}$. This model allows to describe compositions in the range 30.8–53.8 at.% A and assumes full occupancy on sites $6c_1$ and $6c_2$ and null occupancy on site 18*h*.

fails to describe the whole range of existence of the μ phase since Ta richest Ta–Ni μ phase (55 at.% A) stands little outside the range described (at.% A $<$ 53.8) and the Nb–Ni μ phase reaches 56.9 at.% A—the Mn–Si μ phase being well above. While due to the lack of crystallographic information no choice was possible among the three different models proposed by Davydoff and Kattner, the last one is clearly the best in view of the present work.

Those different compound energy models stand among those reviewed by Ansara et al. [7] or by Hari Kumar et al. [24] for the description of the μ phase. None of the other models reviewed describe better the experimental results. This demonstrates the need of a new model if one wishes to describe the phase consistently with the crystallographic information and to be able to describe all the known μ phases with a unique model. We have shown the need to consider different occupancies on the two sites of coordinence 12 (3*a* and 18*h*). Atomic mixing should be considered in the latter one if one wishes to describe the Mn–Si μ phase, but yet the richest compositions in Nb–Ni and Ta–Ni systems. Moreover, incomplete A filling of site $6c_3$ should be considered to be able to describe compositions below 46.2 at.% A like in Mo–Co system. Therefore, the model proposed is $(A,B)_3\ (A)_{12}(A,B)_6(A,B)_{18}$.

This model has three composition variable sites. In an optimization procedure, it gives rise to the evaluation of eight different end-members. The possibility to use FP values for all of them seems a powerful approach [22]. In case this opportunity is not given, a more classical minimisation procedure has to be run but can be difficult in view of the rather large number of parameters. Only two of these end-members ($A_3A_{12}A_6B_{18}$ and $B_3A_{12}A_6B_{18}$) can be considered as the ideal compound depending on the system considered and be assessed quite precisely using experimental data. In most cases, it seems that a constraint imposing a small difference between them as introduced by Hari Kumar et al. [24] is reasonable. The other compounds can either contribute to the non-stoichiometry and be assessed during the minimisation procedure or non-stable at all and can be fixed to a more or less arbitrary value. As being more physically accurate, it is believed that no use of the excess terms should be necessary. If site fractions are measured, those data may be included as experimental parameters in the assessment and compensate the increase

of model parameters. Such an approach is underway in Nb–Ni system, the results of which will be published soon.

5. Conclusion

It is one of the purposes of the Calphad method to describe phases as a function of composition. In the present and past [8] work, the μ phase has been studied in the range 41–86 at.% and the site occupancies of the different sites were determined. Among the 5 sites of the crystal structure, three at least are found to be disordered, none of them, including the two sites of coordination 12, having a similar behaviour. This gives strong evidence that the general rule stating that sites with equivalent coordination should be combined [25] does not apply systematically and should be used with care. This emphasizes the need of more experimental data before establishing accurate models for non-stoichiometric intermetallic phases.

Acknowledgements

The authors wish to acknowledge F. Briaucourt for help with the synthesis and characterization of the samples and E. Leroy for performing the microprobe analyses.

References

[1] Joubert J-M, Percheron-Guégan A. J Alloys Compd 2001;317–318:71–6.
[2] Joubert J-M, Pommier C, Leroy E, Percheron-Guégan A. J Alloys Compd 2003;356/357:442–6.
[3] Arnfelt H, Westgren A. Jernkontorets Annaler 1935;119:185–96.
[4] Kripyakevitch PI, Gladyshevskii EI, Skolozdra RV. Sov Phys—Crystallogr 1968;12(4):525–7.
[5] Kripyakevitch PI, Gladyshevskii EI, Pylaeva EN. Sov Phys—Crystallogr 1962;7(2):165–8.
[6] Wagner V, Conrad M, Harbrecht B. Acta Crystallogr 1995;C51:1241–3.
[7] Ansara I, Chart TG, Fernandez Guillermet A, Hayes FH, Kattner UR, Pettifor DG, Saunders N, Zeng K. Calphad 1997;21(2):171–218.
[8] Joubert J-M, Feutelais Y. Calphad 2002;26(3):427–38.
[9] Gladyshevskii EI, Kripyakevitch PI, Yarmolyuk YP. Inorg Mater 1965;1:996–9.
[10] Gokhale AB, Abbaschian R. J Phase Equilib 1990;11(5):468–80.
[11] Rodríguez-Carvajal J. XV Congress of International Union of Crystallography, Satellite Meeting on Powder Diffraction; 1990. p. 127.
[12] Nash A, Nash P. Bull Alloy Phase Diagrams 1984;5(3):259–65.
[13] Pimenov VN, Ugaste YE, Akkushkarova KA. Izv Akad Nauk SSSR Metally 1977;1(184-189).
[14] Cui Y, Jin Z. Z Metallkde 1999;90(3):233–41.
[15] Davydov A, Kattner UR. J Phase Equilib 1999;20(1):5–16.
[16] Quinn TJ, Hume-Rothery W. J Less-Common Met 1963;5:314–24.
[17] Heijwegen CP, Rieck GD. J Less-Common Met 1974;34:309–14.
[18] Shoemaker CB, Shoemaker DP. Acta Crystallogr 1978;B34:701–5.
[19] Shoemaker CB, Shoemaker DP. Acta Crystallogr 1971;B27:227–35.
[20] Wieser PF, Forgeng WD. Trans Met Soc 1964;230:1675–81.
[21] Sluiter M, Pasturel A, Kawazoe Y. Phys Rev B 2003;67:174203.
[22] Dupin N, Fries SG, Joubert J-M, Sundman B, Sluiter M, Kawazoe Y, Pasturel A. Philos Mag 2004; in press.
[23] Bolcavage A, Kattner UR. J Phase Equilib 1996;17(2):92–100.
[24] Hari Kumar KC, Ansara I, Wollants P. Calphad 1998;22(3):323–34.
[25] Hillert M. Calphad 1998;22(1):127–33.
[26] Massalski TB. Binary alloys phase diagrams, 2nd ed. Materials Park, Ohio: ASM International; 1990.